2019

Synthesis, physical characterization, antifungal and antibacterial activity of oleic acid-capped nanomagnetite and cobalt-doped nanomagnetite

Abbas Rahdar
Department of Physics, University of Zabol

Hamid Beyzaei
Department of Chemistry, University of Zabol

Mohsen Saadat
Department of Physics, University of Sistan and Baluchestan

Xiao Yu
Department of Chemistry and Biochemistry, University of Windsor

John F. Trant
Department of Chemistry and Biochemistry, University of Windsor

Synthesis, physical characterization, antifungal and antibacterial activity of oleic acid-capped nanomagnetite and cobalt-doped nanomagnetite

Abbas Rahdar[1*], Hamid Beyzaei[2], Mohsen Saadat[3], Xiao Yu[4], John F. Trant[4*]

[1] Department of Physics, University of Zabol, Zabol, P. O. Box. 35856-98613, Islamic Republic of Iran

[2] Department of Chemistry, University of Zabol, Zabol, P. O. Box. 35856-98613, Islamic Republic of Iran

[3] Department of Physics, University of Sistan and Baluchestan, Zahedan, Islamic Republic of Iran

[4] Department of Chemistry and Biochemistry, University of Windsor, Windsor, ON, N9B 3P4, Canada

* Corresponding Authors

Email addresses: a.rahdar@uoz.ac.ir; j.trant@uwindsor.ca

Corresponding author for the editorial office:

Dr. John F. Trant

Fax Number: 1-519-973-7098

Phone number: 1-519-253-3000 extension 3528

Abstract

Nanoparticles, 10-14 nm, consisting of either Fe_3O_4 or $Co_{0.2}Fe_{2.8}O_4$ stabilized with oleic acid, were prepared using solution combustion. Their structural and magnetic properties were examined using X-ray diffractometry, scanning electron microscopy, vibrating sample magnetometry, and Fourier-transform infrared spectroscopy. The properties of both sets of materials are similar except the cobalt-doped particles are considerably less magnetic. The *in vitro* inhibitory activities of the nanoparticles were assessed against pathogenic bacteria *Shigella dysenteriae*, *Klebsiella pneumoniae*, *Acinetobacter baumannii*, *Streptococcus pyogenes*, and pathogenic fungi and molds *Candida albicans*, *Fusarium oxysporum* and *Aspergillus fumigatus*. The magnetite nanoparticles were moderately effective against all tested pathogens, but the activity of the cobalt-doped nanoparticles was significantly lower, possibly due to an interruption of the Fenton reaction at the bacterial membrane. This work suggests that potentially doping magnetite with stronger metal oxidants may instead enhance their antimicrobial effects.

Keywords: Magnetic nanoparticles, cobalt-doped magnetite, antifungal activity, antibiotic.

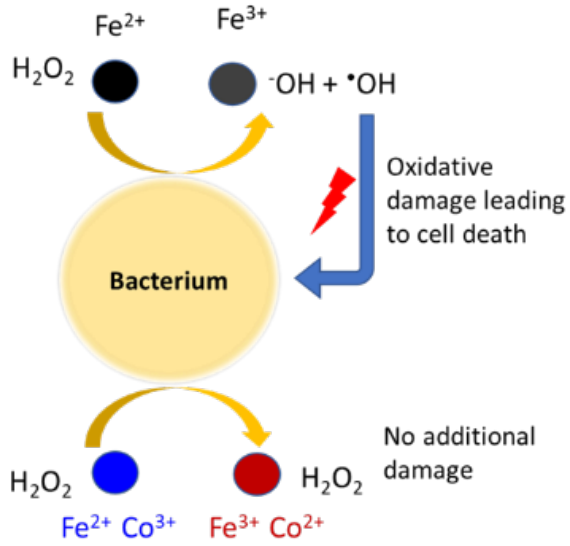
Fe2+
Fe3+
H2O2
-OH + •OH
Oxidative damage leading to cell death
Bacterium
No additional damage
H2O2
H2O2
Fe2+ Co3+
Fe3+ Co2+

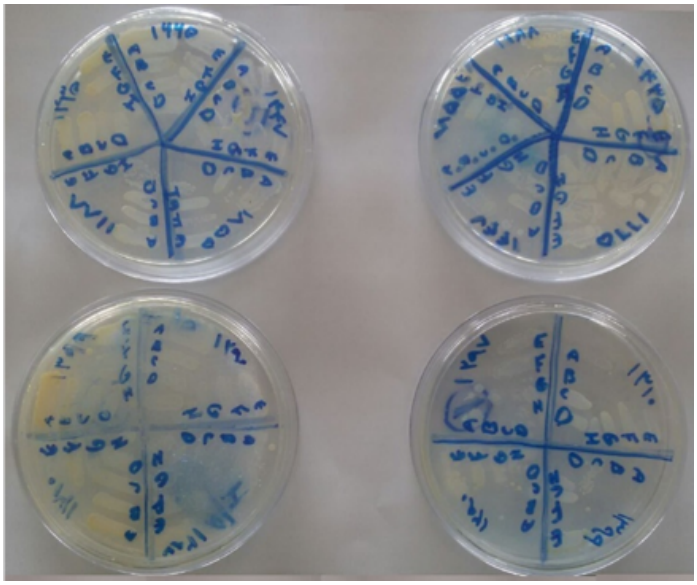

40

1. Introduction

Nanomagnetite, Fe_3O_4 formulated as a nanoparticle, has been used for a variety of biomedical applications including for biosensors,[1] drug delivery,[2-3] hyperthermic therapy,[4] magnetic resonance imaging,[5-7] and medical diagnostics and therapy.[8-11] It is a promising biomedical material due to its high degree of chemical stability, magnetic behaviour, and biocompatibility.[12-19] The physical and magnetic properties can be further tuned through controlled doping with other metals. Cobalt-doping magnetite provides the materials with increased hardness, higher electrical resistivity and higher electrical permeability at higher frequencies.[20-21]

Our previous work with nanomagnetite has focused on using them as antibiotics,[22-26] and there are multiple excellent recent reviews on the subject.[27-28] Nanomagnetite has been extensively studied by others for antibiotic applications as core-shell formulations,[29-30] as uncoated nanoparticles,[31-32] as nanoparticles either doped or combined with other metals,[33-35] or simply as drug delivery vehicles where the antibiotics adsorbed onto the surface.[36] We have previously investigated the antibiotic potential of uncoated magnetite prepared using an additive-free electrochemical approach.[23-26] The surface of these particles incorporated highly oxidized impurities that both inhibited aggregation and were responsible for the potent antibacterial activity. However, we wanted to explore the activity of a more traditional magnetite formulation and help determine whether the activity observed was due to the presence of Fe-O-O-H groups or due to the activity of the magnetite functionality. Doping with different metals might affect the behaviour of the materials; for example, Zn-doped nanomagnetite showed greater activity (defined in terms of inhibition zone diameter) than Fe_3O_4 alone.[37] This activity was ascribed to the increased specific surface area. However, the antibiotic activity of cobalt-doped magnetite has not been extensively studied and the little recent research has largely been restricted to antibacterial behaviour,[38-41] although there are

some notable exceptions: Žalnėravičius and co-workers showed that nanomagnetites with varying cobalt content and capped with L-lysine were potent agents against *E. coli, S. aureus,* and the fungi *C. parapsilosis* and *C. albicans,*[42] and that activity was highly dependent on nanoparticle size and cobalt content.[43] Smaller particles, and less cobalt content was associated with more potent activity.

Antifungal function might prove highly attractive for many consumer products to reduce molds and fungal biofilms.[44] We know that our previously generated nanomagnetites showed very little toxicity towards mammalian cells while being highly toxic to both Gram-negative and Gram-positive bacteria.[23, 25] This selective activity was likely due to the difference in biofilm formation around the nanoparticles, and it is unclear what the activity would be against a eukaryotic fungus.

For this study we are studying the activity against *Shigella dysenteriae*, *Klebsiella pneumoniae*, *Acinetobacter baumannii*, *Streptococcus pyogenes*, and pathogenic fungi and molds *Candida albicans*, *Fusarium oxysporum* and *Aspergillus fumigatus*. These are all high-risk pathogens. *S. dystenteriae,* as implied by the name, releases the Shiga toxins that cause gastroenteritis and can lead to severe complications including renal failure and haemorrhagic colitis.[45] *K. pneumoniae* is a common bacterium previously associated with community-acquired pneumonia,[46] but whose main feature of interest is as the source of carbapenem resistant genes that are spreading to other bacteria and contributing to the antibiotic resistance threat.[47] *A. baumannii* strains resistant to all known antibiotics have been identified and the pathogen is a leading cause of hospital acquired pneumonia and can readily lead to death in already compromised patients.[48] *S. pyogenes*, group A *Streptococcus,* is responsible for many cases of necrotizing fasciitis and is responsible for 160,000 deaths globally each year often through rheumatic fever; fortunately it is still largely susceptible to antibiotic treatment.[49] *C. albicans* is one of the best studied fungal pathogens as it is a near-universally present member

of a healthy human oral microbiome, but one that can, for immunocompromised individuals, cause inflammatory oral candidiasis.[50] It is also the pathogen largely responsible for vulvovaginal "yeast infections" and, if it enters the blood stream, it can often lead to fatal infection. *F. oxysporum* is mainly of interest as a plant pathogen and is responsible for "banana wilt" which is threatening the genetically monodisperse Cavendish banana, the variety most familiar with consumers. There are no effective countermeasures available.[51] *A. fumigatus* is a ubiquitous and extremely thermotolerant mold that emerged as a leading cause of opportunistic fungal infection in humans that has been partially tamed through the use of azole antifungals. Unfortunately, azole-resistant strains have started rapidly spreading around the world in recent years.[52] Together these pathogens threaten human and agricultural health, and many are at the forefront of the antibiotic resistance phenomenon and new classes of therapeutic interventions are required.

Here we report our investigations into the synthesis of nanomagnetite and cobalt-doped nanomagnetite terminated with oleic acid, a common terminating agent,[53-54] and their physical, magnetic, and biological characterization including their activity against these pathogenic bacteria and fungi.

2. Experimental

2.1. Materials and General Methods

Oleic acid hydrate, cobalt nitrate hexahydrate, iron (III) nitrate nonahydrate, iron (II) chloride tetrahydrate, toluene, and sodium hydroxide were purchased from Millipore Sigma and used as received. For the *in vitro* analysis the positive controls ampicillin, gentamicin, terbinafine and canazole were purchased from Millipore Sigma and used as received. Fungal and bacterial culture media including Roswell Park Memorial Institute 1640 (RPMI 1640) medium buffered to pH 7.0 with morpholine propane sulfonic acid (MOPS); Mueller-Hinton

broth (MHB) and Mueller-Hinton agar (MHA), were obtained from HiMedia (Mumbai, India). Gram-negative bacterial strains *Shigella dysenteriae* (PTCC 1188), *Klebsiella pneumoniae* (PTCC 1290), *Acinetobacter baumannii* (PTCC 1855); Gram-positive *Streptococcus pyogenes* (PTCC 1447); pathogenic yeast *Candida albicans* (PTCC 5027); and molds *Fusarium oxysporum* (PTCC 5115) and *Aspergillus fumigatus* (PTCC 5009) were obtained from the Persian Type Culture Collection (Karaj, Iran).

2.2. Synthesis of the Fe_3O_4 and Co/Fe_3O_4 nanoparticles

The oleic acid-capped Fe_3O_4 and Co-doped Fe_3O_4 nanoparticles were prepared using chemical co-precipitation and thermal combustion similar to previously published approaches.[54-55] An aqueous solution was prepared by dissolving iron (II) chloride tetrahydrate (1.00 g, 7.89 mmol) and iron (III) nitrate nonahydrate (5.30 g, 21.9 mmol) in a 1:2 molar ratio in 30 ml of distilled water already containing toluene (40 mL) and oleic acid (1.30 g, 4.60 mmol). The mixture was magnetically stirred at 70 °C to initiate the solution combustion[56] while 4 mL of 25% aqueous ammonia was added in one batch to the solution to increase the pH to 10.5. The mixture is allowed to continue stirring while the reaction occurs. WARNING: Extremely exothermic reaction occurs. The resulting black precipitate was collected by filtration and extensively washed with deionized water; with the material centrifuged at 10000 rpm and the supernatant decanted between each wash, before being dried at 70 °C for 2 h.

The cobalt-doped iron oxide nanoparticles (Co/Fe_3O_4) were prepared in a similar fashion by introducing a controlled amount of cobalt nitrate into the initial solution. In a typical procedure, 0.43 g of $Co(NO_3)_2{\cdot}(H_2O)_6$ was added to iron (II) chloride tetrahydrate (0.56 g) and iron (III) nitrate nonahydrate (5.26 g) in a 1:2 molar ratio in 30 ml of distilled water already containing toluene and oleic acid as described above. The solution was then treated identically to the solution above to provide $Co_{0.2}Fe_{2.8}O_4$.

2.3. Characterization of the Fe_3O_4 and $Co_{0.2}Fe_{2.8}O_4$ nanoparticles

X-ray diffraction (XRD) characterization was conducted on an X'pert Pro MPD (Malvern) X-ray diffractometer equipped with a Cu Kα radiation source. The morphology of the samples was studied using a scanning electron microscope (SEM) and the EDXS spectra and atomic quantification were acquired at the same time (KYKY-EM3900M, Beijing China). Vibrating sample magnetization (VSM) was carried out using an MDKB VSM instrument (Danesh Pajouh Company, Kashan, Iran). FTIR spectroscopy of the nano-structures was conducted by first suspending them in a KBr pellet and then using a 460 PLUS Jasco spectrometer scanning from 400 to 4000 cm^{-1}. All experiments were conducted at ambient temperature (23-25 ºC).

2.4. In vitro inhibitory activities of nanoparticles

Broth microdilution and time-kill methods were applied to assay antimicrobial susceptibility according to the Clinical and Laboratory Standards Institute (CLSI) guidelines M07-A9,[57] M27-A2,[58] M38-A2,[59] and M26-A.[60] The results were the average of three independent experiments. For these experiments, the yeast, mold and bacterial suspensions were prepared in the appropriate broth media (as indicated above) at 0.5-2.5 × 10^3, 0.4-5 × 10^4 and 5 × 10^5 CFU ml^{-1} respectively.[61]

2.4.1. MIC testing

Aliquots of the nanoparticle solutions, 20 µL at a concentration of 20,480 µg ml^{-1} in distilled water, were added to both the first and second wells in each row of a 96-well microliter plate. 20 µl distilled water was added to wells 2-12, and two-fold serial dilutions were carried out in them by transferring 20 µl from the previous well (making the total temporarily 40 µl), mixing thoroughly with the pipette, and adding 20 µl to the next well; for the final well, 20 µl was withdrawn and discarded after mixing. 80 µl of MHB (for bacteria) or RPMI 1640 (for fungi) with 100 µl of the prepared microbial suspensions (see above) were then added to all the wells. This provides, a concentration range of 2048-1 µg ml^{-1} of each derivative in each row. These

165 microliter plates were incubated with shaking at 100 rpm at 37 °C for 24 h. The lowest
166 concentration of derivatives that resulted in no visible turbidity was considered the MIC value.
167 Experiments were repeated on two additional separate occasions with fresh preparations of
168 pathogens. Results from the three experiments were identical.

169 **2.4.2. MBC and MFC testing**

170 Samples of all wells that showed no growth in the MIC test, were cultured in MHA or RPMI
171 1640 agar, which then were incubated at 37 °C for another 24 h. The MBC and MFC was
172 identified as the lowest concentration at which no microbial populations were present.

173 **3. Results and Discussions**

174 **3.1. XRD characterization**

175 The nanoparticles were prepared by mixing Fe (II), and Fe (III) with or without Co (II)
176 in aqueous solution and conducting solution combustion.[56] Under these conditions, the cobalt
177 is oxidized to cobalt (III)[62] during the process and these tetrahedral (as opposed to octahedral
178 Co (II)[63]) are incorporated into the lattice. The resulting particles were characterized by XRD
179 (Figure 1). The spectra are consistent with the reported JCPDS spectra for both samples
180 (JCPDS 003-0863) with Bragg peaks of 30.4° (2 2 0), 35.8° (3 1 1), 43.4° (4 0 0), 53.5° (4 2 2),
181 57.2° (5 1 1), 63.2° (4 4 0) and 74.2° (5 3 3).

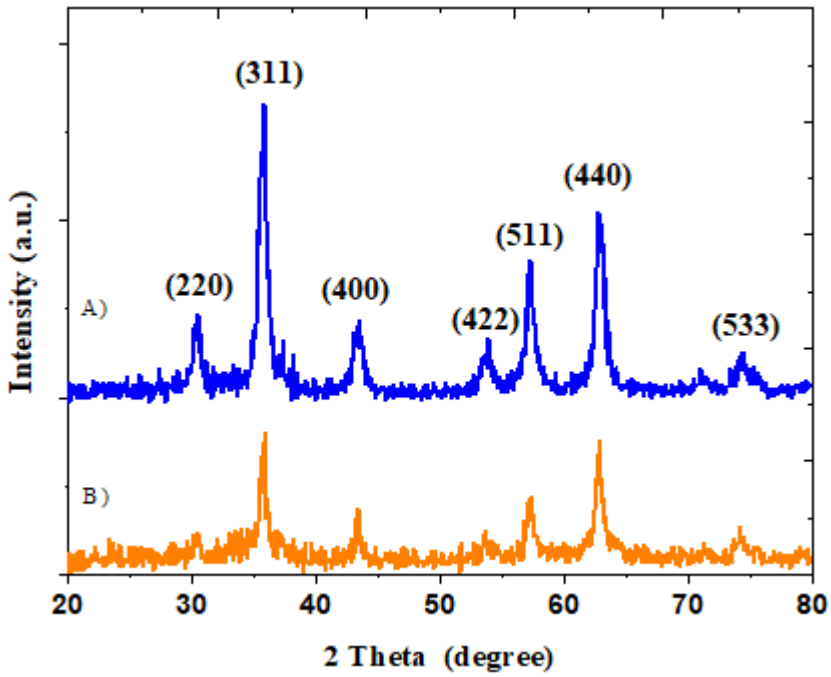

Figure 1. XRD spectra of Fe_3O_4 (A) and $Co_{0.2}Fe_{2.8}O_4$ (B) nanoparticles recorded at 23 °C.

The average crystallite size of the nanostructures was calculated from peak (3 1 1) using the Sherrer formula.[32, 64]

$$D_{h,k,l}=0.9\lambda/(\beta_{h,k,l}\cos\theta) \quad (3)$$

Where λ is the wavelength (λ = 1.542 Å) (CuK_α), β is the product of the full width at half maximum (FWHM) of the selected peak and π/2 as it approximates a Gaussian distribution. θ is the diffraction angle of the peak.

The average crystallite sizes for the nanomagenetite and cobalt-doped nanomagnetite were 14 and 10 nm respectively. The XRD spectra for both samples were similar and could not be used to confirm the presence of cobalt in the crystal.

3.2. Morphological Analysis

SEM was used to support the sizing of the materials (Figure 2), and showed that the structures formed (white spheres on a black matrix background) are roughly spherical and under 100 nm, although the aggregation behaviour under the SEM imaging conditions makes it challenging

to visualize individual particles. Unlike XRD, the energy dispersive X-ray analysis shows clear evidence for the presence of both the cobalt and the iron in the samples and can be used to quantify the relative atomic quantities of the species in the sample using external standards.[65] This method provides the experimental formula of $Co_{0.21}Fe_{2.51}O_{4.28}$ for the batch used for the biological analyses. This is in reasonable agreement with the theoretical formula.

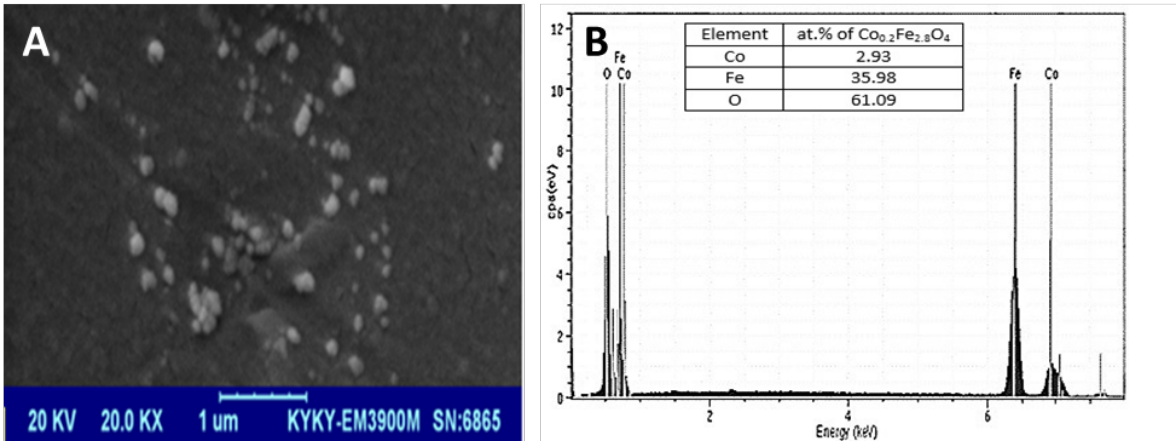

Figure 2. A) A representative SEM image, and B) the EDXS spectrum of the $Co_{0.2}Fe_{2.8}O_4$ nanoparticles.

3.3. FTIR Characterization

The FTIR spectra of both samples are provided as Figure 3.

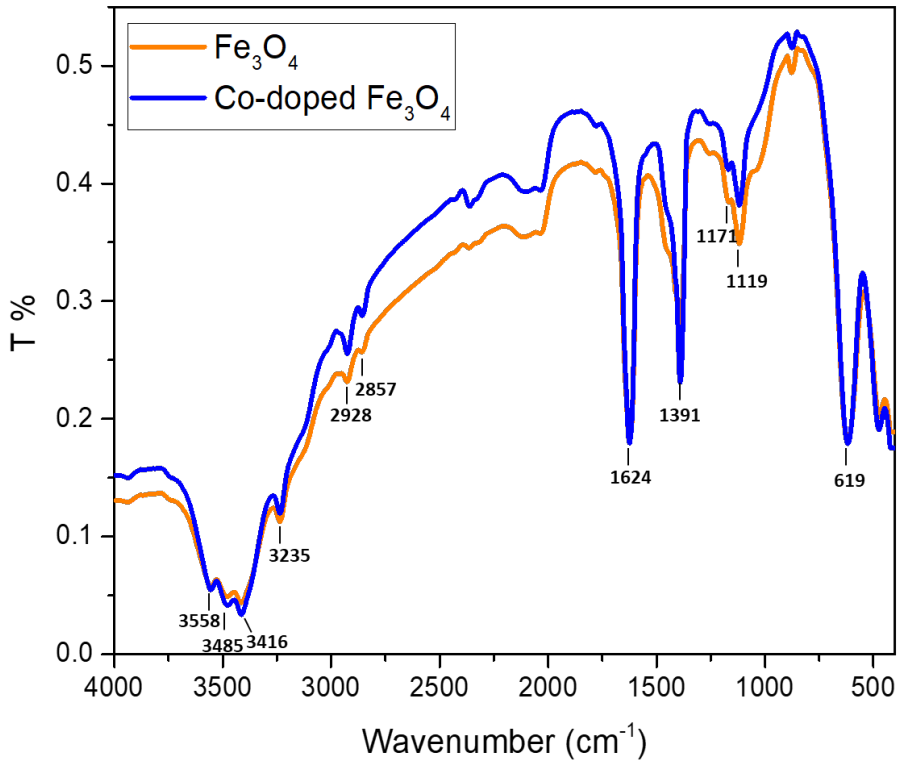

207

208 **Figure 3.** FT-IR spectrum of Fe_3O_4 and Co/ Fe_3O_4 nanoparticles

209 The spectra are largely identical as expected: broad peaks at 3600-3400 cm^{-1} arise from O-H
210 stretching of adsorbed water molecules. The low wavenumber cluster (500-600 cm^{-1}) are
211 expected from the metal-oxygen vibrations, and the strong signal at 1390 cm^{-1} is due to the
212 stretching vibrations in adsorbed nitrate. Vibrations at 1624 cm^{-1} correspond to the vibrations
213 of the C-O of the oleic acid,[37] and the lack of a strong band at 1710 cm^{-1} is consistent with an
214 oleic acid monolayer.[53]

215 ### 3.4. Magnetic Measurements

216 Vibration sample magnetization was used to understand the magnetic behaviour of the
217 materials. They are largely similar under all other characterization techniques, but the doping
218 does have a significant impact on the magnitude of their magnetic behaviour (Figure 4, Table
219 1).

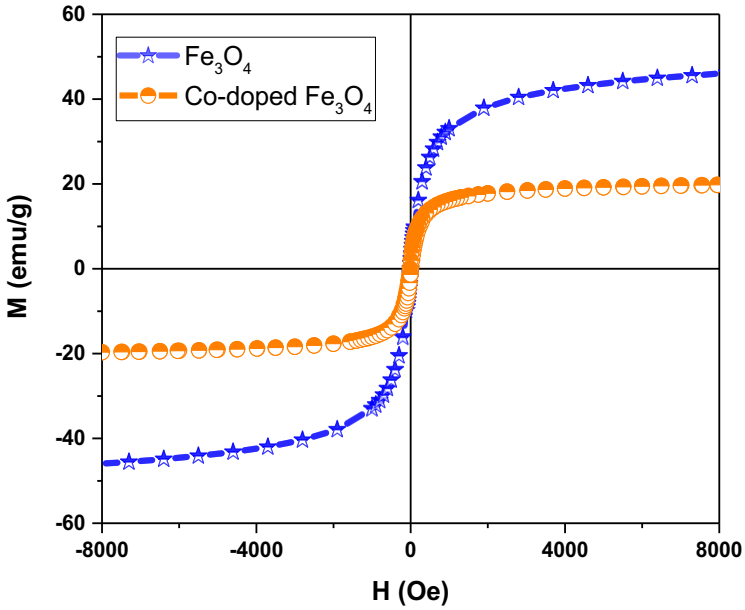

Figure 4. The magnetization loops of Fe_3O_4 and Co-doped Fe_3O_4 nanoparticles, recorded at 23 ºC

Table 1. Effect of Co on magnetic properties of the Fe_3O_4 NPs

Nanoparticles	M_s (emu/gr)	M_r (emu/gr)	H_C (Oe)
Fe_3O_4	44.5	0.2	0.0
Co-doped Fe_3O_4	19.0	1.9	19.3

VSM analysis confirms that the samples are superparamagnetic as expected. The differences in saturation magnetization (M_s), coercivity (H_C), and remnant magnetism (M_r) can be explained based on F-center exchange coupling (FCE) theory.[66-68] Co-doped nanoparticles are more strongly affected by FCE interactions due to the smaller distance between the Co and the Fe ions. This traps electrons in the oxygen vacancy, which acts as a coupling center, and as a result increases the magnetization of the nanoparticles.[29, 35, 37] The magnetization is affected as a consequence of Co concentration within the nano-structure. The small distances between Co

and iron ions are smaller than between iron atoms, and this can lead to trapping an electron in oxygen vacancy, which acts as a coupling center. This results in a change in the magnetization of the nanoparticles as a function of Co content.

3.5. *Evaluation of antimicrobial activity*

The inhibitory potential of nanoparticles was studied against both Gram-negative and Gram-positive bacterial strains as well as some fungal pathogens. Experiments were carried out in solution by using serial dilutions of stock solutions of the nanoparticles added to media inoculated with the pathogen at the appropriate concentration. The results were reported as the minimum inhibitory concentration (MIC) defined as the concentration at which no further increase in solution optical density was observed, the minimum bactericidal concentration (MBC) and the minimum fungicidal concentration (MFC) defined as the concentration at which cell culture on appropriate petri dishes showed no growth (Tables 2 and 3).

Table 2. Antibacterial activity of nanoparticles

		NPs		**Antibiotics**	
Bacteria		Fe_3O_4	$Co_{0.2}Fe_{2.8}O_4$	Ampicillin	Gentamicin
Shigella	MIC	512	>2048	256	0.031
dysenteriae	MBC	1024	>2048	256	0.063
Klebsiella	MIC	512	>2048	32	4
pneumoniae	MBC	512	>2048	64	4
Acinetobacter	MIC	512	>2048	64	16
baumannii	MBC	1024	>2048	128	32
Streptococcus	MIC	1024	>2048	4	2
pyogene	MBC	2048	>2048	8	2

MIC (μg ml^{-1}), MBC (μg ml^{-1})

Table 3. Antifungal activity of nanoparticles

	NPs	**Antifungals**

Fungi		Fe_3O_4	Co-Fe_3O_4	Terbinafine	Canazole
Candida	MIC	2	1024	32	256
albicans	MFC	4	1024	64	512
Fusarium	MIC	128	>2048	32	256
oxysporum	MFC	256	>2048	64	512
Aspergillus	MIC	2	256	32	32
fumigatus	MFC	1	256	32	32

MIC (μg ml^{-1}), MFC (μg ml^{-1}

The unmodified magnetite nanoparticles efficiently blocked the growth of all bacterial and fungal pathogens; however, these oleic acid-capped compounds were not as effective as our previously reported uncapped, surfactant-free particles which showed MICs of 2.0 μg/ml against *S. aureus* and *E. coli*.[25] The Co-doped Fe_3O_4 nanoparticles showed no antibacterial activity. This difference in activity could be ascribed to the mechanism of action of these capped nanomagnetites compared to our previous systems.

The particles bind to the plasma membrane of the pathogens causing additional membrane disruption and ensuring that the generated reactive oxidative species are already co-localized to the lipids.[28] The generally accepted mechanism of action for the antibacterial activity of capped-magnetite is through the conversion of endogenous hydrogen peroxide into more reactive oxygen species (ROS, superoxide, hydroxyl radical, proxy radical) that readily cause cellular damage through non-specific oxidation of the lipid membrane.[69-70] This occurs through the slow oxidation of the magnetite (Fe_3O_4), which contains a mixture of Fe^{2+} and Fe^{3+} ions, to maghemite (γ-Fe_2O_3) through the Fenton reaction as the Fe (II) atoms slowly oxidize to the more stable Fe (III) (Figure 5).[71] However, this may become more complicated in the presence of the cobalt (III). As the electron is released from the iron atom it could be trapped by the Co (III) to revert it to the highly stable Co (II). This would prevent the formation of the

highly oxidized species. Further investigations are required to explore and confirm this mechanism of action.

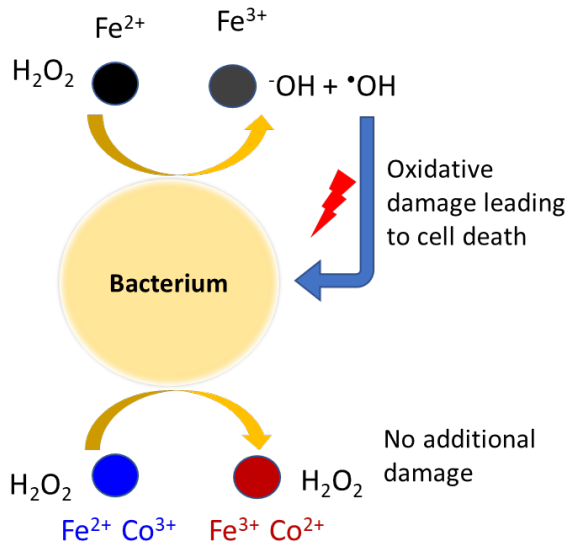

Figure 5. Schematic of the mechanism of action of the iron oxide nanoparticles, and a proposed mode of action for the cobalt-doped nanomagnetite as a possible cause of the lack of antibacterial activity of the cobalt-doped nanoparticles.

In contrast, the magnetite was observed to be quite a potent antifungal with lower MICs and MFCs lower than front-line antifungals terbinafine and canazole.[72-73] The cobalt-doped materials show some slight activity. To contextualize these results, the activity is considerably better than that observed by Seddighi and their larger iron oxide nanoparticles.[31] They observed MFCs of between 500-1000 µg/mL for particles 30-40 nm in diameter (ours are closer to 14 nm). The smaller particles are expected to be more effective as the cytotoxic ROS production is a function of surface area. Anghel and co-workers used similar oleic acid-coated magnetite nanoparticles to inhibit fungal growth on textiles, but do not report the size of the particles to allow for direct comparison.[44] Žalnėravičius and co-workers carried out two studies using cobalt-doped magnetite as antifungal agents. However, they did not compare the efficacy of the particles against antifungals and report the exclusion diameter rather than an MIC and so it

is hard to compare the results to the current study.[42-43] In their work, smaller particles were found to be more active, magnetite was found to be more active than cobalt-doped magnetite, and antimicrobial activity decreased as cobalt content increased. This is consistent with our current results and is possibly explainable by the decreased production of ROS. Doping the magnetite with stronger oxidants than Fe (II) might invert this attenuation of activity. Regardless, this magnetite is considerably less active against bacteria compared to our previously prepared uncapped magnetite which has not been evaluated against fungi to date; unsurprisingly, masking the surface of the metal nanoparticle decreases their activity.

6. Conclusion

Nanomagnetite (Fe_3O_4) and Co-doped nanomagnetite ($Co_{0.2}Fe_{2.8}O_4$) stabilized with oleic acid were synthesized via co-precipitation with diameters of ~10–14 nm. The two sets of materials showed similar physical characterization, but the cobalt-doped materials were considerably less magnetic. They also differed greatly in biological activity: the oleic acid-terminated nanomagnetite is a potent antibacterial and very potent antifungal. Introducing cobalt greatly decreases their antibiotic activity. The introduction of stronger metal oxidants than Fe (II) such as copper, tin, chrome, zinc and magnesium may improve their antimicrobial effects.

Acknowledgments

A. Rahdar would like to thank the University of Zabol for financial support (UOZ-GR-9618-40) for this work. JFT gratefully acknowledges financial support from the University of Windsor (JFT grant no 817074), the Natural Sciences and Engineering Research Council of Canada (JFT grant no 2018-06338). The authors declare no competing financial interests.

References

1. Kairdolf, B. A.; Qian, X.; Nie, S., Bioconjugated nanoparticles for biosensing, *in vivo* imaging, and medical diagnostics. *Anal. Chem.* **2017,** *89* (2), 1015-1031. DOI: http://doi.org/10.1021/acs.analchem.6b04873

2. Skorjanc, T.; Benyettou, F.; Olsen, J.-C.; Trabolsi, A., Design of organic macrocycle-modified iron oxide nanoparticles for drug delivery. *Chem. - Eur. J.* **2017,** *23* (35), 8333-8347. DOI: http://doi.org/10.1002/chem.201605246

3. El-Boubbou, K., Magnetic iron oxide nanoparticles as drug carriers: Clinical relevance. *Nanomedicine* **2018,** *13* (8), 953-971. DOI: http://doi.org/10.2217/nnm-2017-0336

4. Tebaldi, M. L.; Oda, C. M. R.; Monteiro, L. O. F.; de Barros, A. L. B.; Santos, C. J.; Soares, D. C. F., Biomedical nanoparticle carriers with combined thermal and magnetic response: Current preclinical investigations. *J. Magn. Magn. Mater.* **2018,** *461*, 116-127. DOI: http://doi.org/10.1016/j.jmmm.2018.04.032

5. Shen, Z.; Wu, A.; Chen, X., Iron oxide nanoparticle based contrast agents for magnetic resonance imaging. *Mol. Pharmaceutics* **2017,** *14* (5), 1352-1364. DOI: http://doi.org/10.1021/acs.molpharmaceut.6b00839

6. Wáng, Y. X. J.; Idée, J.-M., A comprehensive literatures update of clinical researches of superparamagnetic resonance iron oxide nanoparticles for magnetic resonance imaging. *Quant. Imaging Med. Surg.* **2017,** *7* (1), 88-122. DOI: http://doi.org/10.21037/qims.2017.02.09

7. Bao, Y.; Sherwood, J. A.; Sun, Z., Magnetic iron oxide nanoparticles as T_1 contrast agents for magnetic resonance imaging. *J. Mater. Chem. C* **2018,** *6* (6), 1280-1290. DOI: http://doi.org/10.1039/c7tc05854c

8. Saeed, M.; Ren, W.; Wu, A., Therapeutic applications of iron oxide based nanoparticles in cancer: Basic concepts and recent advances. *Biomater. Sci.* **2018,** *6* (4), 708-725. DOI: http://doi.org/10.1039/c7bm00999b

9. Hu, Y.; Mignani, S.; Majoral, J.-P.; Shen, M.; Shi, X., Construction of iron oxide nanoparticle-based hybrid platforms for tumor imaging and therapy. *Chem. Soc. Rev.* **2018,** *47* (5), 1874-1900. DOI: http://doi.org/10.1039/c7cs00657h

10. Qian, X.; Han, X.; Chen, Y., Insights into the unique functionality of inorganic micro/nanoparticles for versatile ultrasound theranostics. *Biomaterials* **2017,** *142*, 13-30. DOI: http://doi.org/10.1016/j.biomaterials.2017.07.016

11. Shabestari Khiabani, S.; Farshbaf, M.; Akbarzadeh, A.; Davaran, S., Magnetic nanoparticles: preparation methods, applications in cancer diagnosis and cancer therapy. *Artif. Cells, Nanomed., Biotechnol.* **2017,** *45* (1), 6-17. DOI: http://doi.org/10.3109/21691401.2016.1167704

12. Mohammed, L.; Gomaa, H. G.; Ragab, D.; Zhu, J., Magnetic nanoparticles for environmental and biomedical applications: A review. *Particuology* **2017,** *30*, 1-14. DOI: http://doi.org/10.1016/j.partic.2016.06.001

13. Frey, N. A.; Peng, S.; Cheng, K.; Sun, S., Magnetic nanoparticles: Synthesis, functionalization, and applications in bioimaging and magnetic energy storage. *Chem. Soc. Rev.* **2009,** *38* (9), 2532-2542. DOI: http://doi.org/10.1039/b815548h

14. Su, C., Environmental implications and applications of engineered nanoscale magnetite and its hybrid nanocomposites: A review of recent literature. *J. Hazard. Mater.* **2016,** *322* (Part A), 48-84. DOI: http://doi.org/10.1016/j.jhazmat.2016.06.060

15. Shan, J.; Wang, L.; Yu, H.; Ji, J.; Amer, W. A.; Chen, Y.; Jing, G.; Khalid, H.; Akram, M.; Abbasi, N. M., Recent progress in Fe_3O_4 based magnetic nanoparticles: From synthesis to application. *Mater. Sci. Technol.* **2016,** *32* (6), 602-614. DOI: http://doi.org/10.1179/1743284715y.0000000122

16. Nguyen, V. L.; Yang, Y.; Teranishi, T.; Thi, C. M.; Cao, Y.; Nogami, M., Biomedical applications of advanced multifunctional magnetic nanoparticles. *J. Nanosci. Nanotechnol.* **2015,** *15* (12), 10091-10107. DOI: http://doi.org/10.1166/jnn.2015.11691

17. Xu, J.-K.; Zhang, F.-F.; Sun, J.-J.; Sheng, J.; Wang, F.; Sun, M., Bio and nanomaterials based on Fe_3O_4. *Molecules* **2014,** *19* (12), 21506-21528. DOI: http://doi.org/10.3390/molecules191221506

18. Gawande, M. B.; Branco, P. S.; Varma, R. S., Nano-magnetite (Fe_3O_4) as a support for recyclable catalysts in the development of sustainable methodologies. *Chem. Soc. Rev.* **2013,** *42*, 3371-3393. DOI: http://doi.org/10.1039/c3cs35480f

19. Müller, S., Magnetic fluid hyperthermia therapy for malignant brain tumors—An ethical discussion. *Nanomed.: Nanotechnol. Biol. Med.* **2009,** *5* (4), 387-393. DOI: http://doi.org/10.1016/j.nano.2009.01.011

20. Sun, S.; Zeng, H.; Robinson, D. B.; Raoux, S.; Rice, P. M.; Wang, S. X.; Li, G., Monodisperse MFe_2O_4 (M = Fe, Co, Mn) nanoparticles. *J. Am. Chem. Soc.* **2004,** *126* (1), 273-279. DOI: http://doi.org/10.1021/ja0380852

21. Yu, Y.; Mendoza-Garcia, A.; Ning, B.; Sun, S., Cobalt-substituted magnetite nanoparticles and their assembly into ferrimagnetic nanoparticle arrays. *Adv. Mater. (Weinheim, Ger.)* **2013,** *25* (22), 3090-3094. DOI: http://doi.org/10.1002/adma.201300595

22. Aliahmad, M.; Rahdar, A.; Sadeghfar, F.; Bagheri, S.; Hajinezhad, M. R., Synthesis and biochemical effects of magnetite nanoparticle by surfactant-free electrochemical method in an aqueous system:the current density effect. *Nanomed. Res. J.* **2016,** *1* (1), 39-46. DOI: http://doi.org/10.7508/nmrj.2016.01.006

23. Rahdar, A.; Taboada, P.; Aliahmad, M.; Hajinezhad, M. R.; Sadeghfar, F., Iron oxide nanoparticles: Synthesis, physical characterization, and intraperitoneal biochemical studies in *Rattus norvegicus*. *J. Mol. Struct.* **2018,** *1173*, 240-245. DOI: http://doi.org/10.1016/j.molstruc.2018.06.098

24. Rahdar, S.; Rahdar, A.; Trant, J. F., Adsorption of bovine serum albumin (BSA) by bare magnetite nanoparticles with surface oxidative impurities that prevent aggregation. *Can. J. Chem.* **2019,** *97*, Early View. DOI: http://doi.org/10.1139/cjc-2019-0008

25. Taimoory, S. M.; Rahdar, A.; Aliahmad, M.; Sadeghfar, F.; Hajinezhad, M. R.; Jahantigh, M.; Shahbazi, P.; Trant, J. F., The synthesis and characterization of a magnetite

nanoparticle with potent antibacterial activity and low mammalian toxicity. *J. Mol. Liq.* **2018,** *265*, 96-104. DOI: http://doi.org/10.1016/j.molliq.2018.05.105

26. Taimoory, S. M.; Rahdar, A.; Aliahmad, M.; Sadeghfar, F.; Hashemzaei, M.; Trant, J. F., Importance of the inter-electrode distance for the electrochemical synthesis of magnetite nanoparticles: Synthesis, characterization, and cytotoxicity. *e-J. Surf. Sci. Nanotechnol.* **2017,** *15*, 31-39. DOI: http://doi.org/10.1380/ejssnt.2017.31

27. Sangaiya, P.; Jayaprakash, R., A review on iron oxide nanoparticles and their biomedical applications. *J. Supercond. Novel Magn.* **2018,** *31* (11), 3397-3413. DOI: http://doi.org/10.1007/s10948-018-4841-2

28. Niemirowicz, K.; Durnaś, B.; Piktel, E.; Bucki, R., Development of antifungal therapies using nanomaterials. *Nanomedicine* **2017,** *12* (15), 1891-1905. DOI: http://doi.org/10.2217/nnm-2017-0052

29. Limban, C.; Missir, A. V.; Caproiu, M. T.; Grumezescu, A. M.; Chifiriuc, M. C.; Bleotu, C.; Marutescu, L.; Papacocea, M. T.; Nuta, D. C., Novel hybrid formulations based on thiourea derivatives and Core@Shell Fe_3O_4@C_{18} nanostructures for the development of antifungal strategies. *Nanomaterials* **2018,** *8* (1), 47. DOI: http://doi.org/10.3390/nano8010047

30. Arakha, M.; Pal, S.; Samantarrai, D.; Panigrahi, T. K.; Mallick, B. C.; Pramanik, K.; Mallick, B.; Jha, S., Antimicrobial activity of iron oxide nanoparticle upon modulation of nanoparticle-bacteria interface. *Sci. Rep.* **2015,** *5*, 14813. DOI: http://doi.org/10.1038/srep14813

31. Seddighi, N. S.; Salari, S.; Izadi, A. R., Evaluation of antifungal effect of iron-oxide nanoparticles against different *Candida* species. *IET Nanobiotechnol.* **2017,** *11* (7), 883-888. DOI: http://doi.org/10.1049/iet-nbt.2017.0025

32. Ansari, S. A.; Oves, M.; Satar, R.; Khan, A.; Ahmad, S. I.; Jafri, M. A.; Zaidi, S. K.; Alqahtani, M. H., Antibacterial activity of iron oxide nanoparticles synthesized by co-precipitation technology against *Bacillus cereus* and *Klebsiella pneumoniae*. *Pol. J. Chem. Technol.* **2017,** *19* (4), 110. DOI: http://doi.org/10.1515/pjct-2017-0076

33. Lazić, V.; Mihajlovski, K.; Mraković, A.; Illés, E.; Stoiljković, M.; Ahrenkiel, S. P.; Nedeljković, J. M., Antimicrobial activity of silver nanoparticles supported by magnetite. *ChemistrySelect* **2019,** *4* (14), 4018-4024. DOI: http://doi.org/10.1002/slct.201900628

34. Prucek, R.; Tuček, J.; Kilianová, M.; Panáček, A.; Kvítek, L.; Filip, J.; Kolář, M.; Tománková, K.; Zbořil, R., The targeted antibacterial and antifungal properties of magnetic nanocomposite of iron oxide and silver nanoparticles. *Biomaterials* **2011,** *32* (21), 4704-4713. DOI: http://doi.org/10.1016/j.biomaterials.2011.03.039

35. Chang, M.; Lin, W.-S.; Xiao, W.; Chen, Y.-N., Antibacterial effects of magnetically-controlled Ag/Fe_3O_4 nanoparticles. *Materials* **2018,** *11* (5), 659. DOI: http://doi.org/10.3390/ma11050659

36. Santos, C. M. B.; da Silva, S. W.; Guilherme, L. R.; Morais, P. C., SERRS study of molecular arrangement of amphotericin B adsorbed onto iron oxide nanoparticles precoated

421 with a bilayer of lauric acid. *J. Phys. Chem. C* **2011,** *115* (42), 20442-20448. DOI:
422 http://doi.org/10.1021/jp206434j

423 37. Anjana, P. M.; Bindhu, M. R.; Umadevi, M.; Rakhi, R. B., Antimicrobial,
424 electrochemical and photo catalytic activities of Zn doped Fe_3O_4 nanoparticles. *J. Mater. Sci.:*
425 *Mater. Electron.* **2018,** *29* (7), 6040-6050. DOI: http://doi.org/10.1007/s10854-018-8578-2

426 38. Venkatesan, K.; Rajan Babu, D.; Kavya Bai, M. P.; Supriya, R.; Vidya, R.;
427 Madeswaran, S.; Anandan, P.; Arivanandhan, M.; Hayakawa, Y., Structural and magnetic
428 properties of cobalt-doped iron oxide nanoparticles prepared by solution combustion method
429 for biomedical applications. *Int. J. Nanomedicine* **2015,** *1*, 189-98. DOI:
430 http://doi.org/10.2147/IJN.S82210

431 39. Sanpo, N.; Berndt, C. C.; Wang, J., Microstructural and antibacterial properties of zinc-
432 substituted cobalt ferrite nanopowders synthesized by sol-gel methods. *J. Appl. Phys.* **2012,**
433 *112* (8), 084333. DOI: http://doi.org/10.1063/1.4761987

434 40. Sanpo, N.; Berndt, C. C.; Wen, C.; Wang, J., Transition metal-substituted cobalt ferrite
435 nanoparticles for biomedical applications. *Acta Biomater.* **2013,** *9* (3), 5830-5837. DOI:
436 http://doi.org/10.1016/j.actbio.2012.10.037

437 41. Samavati, A.; F. Ismail, A., Antibacterial properties of copper-substituted cobalt ferrite
438 nanoparticles synthesized by co-precipitation method. *Particuology* **2017,** *30*, 158-163. DOI:
439 http://doi.org/10.1016/j.partic.2016.06.003

440 42. Žalnėravičius, R.; Paškevičius, A.; Mažeika, K.; Jagminas, A., Fe(II)-substituted cobalt
441 ferrite nanoparticles against multidrug resistant microorganisms. *Appl. Surf. Sci.* **2018,** *435*,
442 141-148. DOI: http://doi.org/10.1016/j.apsusc.2017.11.028

443 43. Žalnėravičius, R.; Paškevičius, A.; Kurtinaitiene, M.; Jagminas, A., Size-dependent
444 antimicrobial properties of the cobalt ferrite nanoparticles. *J. Nanopart. Res.* **2016,** *18* (10),
445 300. DOI: http://doi.org/10.1007/s11051-016-3612-x

446 44. Anghel, I.; Grumezescu, A. M.; Andronescu, E.; Anghel, A. G.; Ficai, A.; Saviuc, C.;
447 Grumezescu, V.; Vasile, B. S.; Chifiriuc, M. C., Magnetite nanoparticles for functionalized
448 textile dressing to prevent fungal biofilms development. *Nanoscale Res. Lett.* **2012,** *7* (1), 501.
449 DOI: http://doi.org/10.1186/1556-276x-7-501

450 45. O'Loughlin, E. V.; Robins-Browne, R. M., Effect of shiga toxin and shiga-like toxins
451 on eukaryotic cells. *Microbes Infect.* **2001,** *3* (6), 493-507. DOI: http://doi.org/10.1016/S1286-
452 4579(01)01405-8

453 46. Tzouvelekis, L. S.; Markogiannakis, A.; Psichogiou, M.; Tassios, P. T.; Daikos, G. L.,
454 Carbapenemases in *Klebsiella pneumoniae* and other *Enterobacteriaceae*: An evolving crisis
455 of global dimensions. *Clin. Microbiol. Rev.* **2012,** *25* (4), 682-707. DOI:
456 http://doi.org/10.1128/cmr.05035-11

457 47. Nordmann, P.; Cuzon, G.; Naas, T., The real threat of *Klebsiella pneumoniae*
458 carbapenemase-producing bacteria. *Lancet Infect. Dis.* **2009,** *9* (4), 228-236. DOI:
459 http://doi.org/10.1016/S1473-3099(09)70054-4

460 48. Peleg, A. Y.; Seifert, H.; Paterson, D. L., *Acinetobacter baumannii*: Emergence of a
461 successful pathogen. *Clin. Microbiol. Rev.* **2008,** *21* (3), 538-582. DOI:
462 http://doi.org/10.1128/cmr.00058-07

463 49. Cole, J. N.; Barnett, T. C.; Nizet, V.; Walker, M. J., Molecular insight into invasive
464 group A streptococcal disease. *Nat. Rev. Microbiol.* **2011,** *9* (10), 724-736. DOI:
465 http://doi.org/10.1038/nrmicro2648

466 50. Mayer, F. L.; Wilson, D.; Hube, B., *Candida albicans* pathogenicity mechanisms.
467 *Virulence* **2013,** *4* (2), 119-128. DOI: http://doi.org/10.4161/viru.22913

468 51. Ploetz, R. C., Management of *Fusarium* wilt of banana: A review with special reference
469 to tropical race 4. *Crop Prot.* **2015,** *73*, 7-15. DOI: http://doi.org/10.1016/j.cropro.2015.01.007

470 52. Verweij, P. E.; Chowdhary, A.; Melchers, W. J. G.; Meis, J. F., Azole resistance in
471 *Aspergillus fumigatus*: Can we retain the clinical use of mold-active antifungal azoles? *Clin.*
472 *Infect. Dis.* **2016,** *62* (3), 362-368. DOI: http://doi.org/10.1093/cid/civ885

473 53. Yang, K.; Peng, H.; Wen, Y.; Li, N., Re-examination of characteristic FTIR spectrum
474 of secondary layer in bilayer oleic acid-coated Fe_3O_4 nanoparticles. *Appl. Surf. Sci.* **2010,** *256*
475 (10), 3093-3097. DOI: http://doi.org/10.1016/j.apsusc.2009.11.079

476 54. Soares, P. I. P.; Laia, C. A. T.; Carvalho, A.; Pereira, L. C. J.; Coutinho, J. T.; Ferreira,
477 I. M. M.; Novo, C. M. M.; Borges, J. P., Iron oxide nanoparticles stabilized with a bilayer of
478 oleic acid for magnetic hyperthermia and MRI applications. *Appl. Surf. Sci.* **2016,** *383*, 240-
479 247. DOI: http://doi.org/10.1016/j.apsusc.2016.04.181

480 55. Gnanaprakash, G.; Philip, J.; Jayakumar, T.; Raj, B., Effect of digestion time and alkali
481 addition rate on physical properties of magnetite nanoparticles. *J. Phys. Chem. B* **2007,** *111*
482 (28), 7978-7986. DOI: http://doi.org/10.1021/jp071299b

483 56. Varma, A.; Mukasyan, A. S.; Rogachev, A. S.; Manukyan, K. V., Solution combustion
484 synthesis of nanoscale materials. *Chem. Rev.* **2016,** *116* (23), 14493-14586. DOI:
485 http://doi.org/10.1021/acs.chemrev.6b00279

486 57. Institute, C. a. L. S., Methods for dilution: Antimicrobial susceptibility tests for bacteria
487 that grow aerobically. Clinical and Laboratory Standards Institute: Wayne, PA, 2018; Vol.
488 CLSI Standard M07-A9.

489 58. Institute, C. a. L. S., Reference method for broth dilution: Antifungal susceptibility
490 testing of yeasts. Clinical and Laboratory Standards Institute: Wayne, PA, 2017; Vol. CLSI
491 Standard M27-A2.

492 59. Institute, C. a. L. S., Reference method for broth dilution: Antifungal susceptibility
493 testing of filamentous fungi. Clinical and Laboratory Standards Institute: Wayne, PA, 2017;
494 Vol. CLSI Standard M38-A2.

495 60. Institute, C. a. L. S., Methods for determining bactericidal activity of antimicrobial
496 agents; Approved guideline. Clinical and Laboratory Standards Institute: Wayne, PA, 1999;
497 Vol. CLSI Standard M26-A.

61. Beyzaei, H.; Kamali Deljoo, M.; Aryan, R.; Ghasemi, B.; Zahedi, M. M.; Moghaddam-Manesh, M., Green multicomponent synthesis, antimicrobial and antioxidant evaluation of novel 5-amino-isoxazole-4-carbonitriles. *Chem. Cent. J.* **2018,** *12* (1), 114. DOI: http://doi.org/10.1186/s13065-018-0488-0

62. Norkus, E.; Vaškelis, A.; Grigucevičienė, A.; Rozovskis, G.; Reklaitis, J.; Norkus, P., Oxidation of cobalt(II) with air oxygen in aqueous ethylenediamine solutions. *Transition Met. Chem. (Dordrecht, Neth.)* **2001,** *26* (4), 465-472. DOI: http://doi.org/10.1023/a:1011051222928

63. Gargallo-Caballero, R.; Martín-García, L.; Quesada, A.; Granados-Miralles, C.; Foerster, M.; Aballe, L.; Bliem, R.; Parkinson, G. S.; Blaha, P.; Marco, J. F.; de la Figuera, J., Co on Fe_3O_4(001): Towards precise control of surface properties. *J. Chem. Phys.* **2016,** *144* (9), 094704. DOI: http://doi.org/10.1063/1.4942662

64. Sun, X. J.; Liu, F. T.; Jiang, Q. H., Synthesis and characterization of Co^{2+}-doped Fe_3O_4 nanoparticles by the solvothermal method. *Mater. Sci. Forum* **2011,** *688*, 364-369. DOI: http://doi.org/10.4028/www.scientific.net/MSF.688.364

65. Koksal, O. K.; Wrobel, P.; Apaydin, G.; Cengiz, E.; Lankosz, M.; Tozar, A.; Karahan, I. H.; Özkalayci, F., Elemental analysis for iron, cobalt, copper and zinc decorated hydroxyapatite synthetic bone dusts by EDXRF and SEM. *Microchem. J.* **2019,** *144*, 83-87. DOI: http://doi.org/10.1016/j.microc.2018.08.050

66. Coey, J. M. D.; Venkatesan, M.; Fitzgerald, C. B., Donor impurity band exchange in dilute ferromagnetic oxides. *Nat. Mater.* **2005,** *4* (2), 173-179. DOI: http://doi.org/10.1038/nmat1310

67. Phokha, S.; Prabhakaran, D.; Boothroyd, A.; Pinitsoontorn, S.; Maensiri, S., Ferromagnetic induced in Cr-doped CeO_2 particles. *Microelectron. Eng.* **2014,** *126*, 93-98. DOI: http://doi.org/10.1016/j.mee.2014.06.028

68. Kumar, S.; Kim, Y. J.; Koo, B. H.; Lee, C. G., Structural and magnetic properties of Ni-doped CeO_2 nanoparticles. *J. Nanosci. Nanotechnol.* **2010,** *10* (11), 7204-7207. DOI: http://doi.org/10.1166/jnn.2010.2751

69. Voinov, M. A.; Pagán, J. O. S.; Morrison, E.; Smirnova, T. I.; Smirnov, A. I., Surface-mediated production of hydroxyl radicals as a mechanism of iron oxide nanoparticle biotoxicity. *J. Am. Chem. Soc* **2011,** *133* (1), 35-41. DOI: http://doi.org/10.1021/ja104683w

70. Fu, P. P.; Xia, Q.; Hwang, H.-M.; Ray, P. C.; Yu, H., Mechanisms of nanotoxicity: Generation of reactive oxygen species. *J. Food Drug Anal.* **2014,** *22* (1), 64-75. DOI: http://doi.org/10.1016/j.jfda.2014.01.005

71. Auffan, M.; Rose, J.; Wiesner, M. R.; Bottero, J.-Y., Chemical stability of metallic nanoparticles: A parameter controlling their potential cellular toxicity *in vitro*. *Environ. Pollut. (Oxford, U. K.)* **2009,** *157* (4), 1127-1133. DOI: http://doi.org/10.1016/j.envpol.2008.10.002

72. Albengres, E.; Le Louët, H.; Tillement, J.-P., Systemic antifungal agents. *Drug Safety* **1998,** *18* (2), 83-97. DOI: http://doi.org/10.2165/00002018-199818020-00001

537 73. Gupta, A. K.; Foley, K. A.; Versteeg, S. G., New antifungal agents and new
538 formulations against dermatophytes. *Mycopathologia* **2017,** *182* (1), 127-141. DOI:
539 http://doi.org/10.1007/s11046-016-0045-0

540

541